Tin Whisker Electrical Short Circuit Characteristics—Part I

Karim J. Courey, Shihab S. Asfour, Jon A. Bayliss, Lawrence L. Ludwig, and Maria C. Zapata

***Abstract*—Existing risk simulations make the assumption that when a free tin whisker has bridged two adjacent exposed electrical conductors, the result is an electrical short circuit. This conservative assumption is made because shorting is a random event that has a currently unknown probability associated with it. Due to contact resistance, electrical shorts may not occur at lower voltage levels. In this experiment, we study the effect of varying voltage on the breakdown of the contact resistance which leads to a short circuit. From this data, we can estimate the probability of an electrical short, as a function of voltage, given that a free tin whisker has bridged two adjacent exposed electrical conductors. In addition, three tin whiskers grown from the same Space Shuttle Orbiter card guide used in the aforementioned experiment were cross sectioned and studied using a focused ion beam (FIB).**

***Index Terms*—Contact resistance, focused ion beam (FIB), short circuit, tin whiskers.**

I. Introduction

METAL whiskers are filamentary growths which may develop on metal surfaces [1]. Metal whiskers usually erupt from thin metal films that have been deposited on a substrate and can grow in a variety of shapes including, straight, kinked, and curved [2]. Metal whiskers have grown on different metal films. Although a number of metal coatings have exhibited a propensity for whisker growth, the metal films that are most often referred to in the metal whisker literature are cadmium [3], zinc, and tin [4]. Tin films deposited by electroplating are more prone to whiskering than hot-dipped coatings [5].

The physical dimensions of tin whiskers also exhibit a great deal of variability. Tin whisker diameters can range from 0.006 to 10 μm [6]. They can also grow up to 18 mm in length [7].

The maximum current that a whisker can carry before fusing open has been measured up to 10 mA for whiskers with a 1-μm diameter, up to 30 mA for whiskers with a 2.5-μm diameter, and up to 75 mA for whiskers with a 4-μm diameter [8]. Given the current-carrying capacity and the length that whiskers can grow, the potential for short circuits in electronics is a very real concern.

The failure modes caused by tin whiskers can be grouped into four different categories. The failure modes include: permanent short circuits in low-current applications, transient short circuits in applications were current is high enough to cause the whisker to fuse open, metal vapor arcing in a vacuum, and debris/contamination resulting from vibration which frees loose whiskers that can interfere with optical surfaces or bridge exposed electrical conductors [9].

Metal whisker failures can be categorized by application into commercial satellite, military, medical, industrial/power, and computers [10]. These failures include heart pacemakers [11], apnea monitors [12], a nuclear reactor shutdown [13], computers in data centers with raised flooring [14], F-15 radar problems [15], Patriot Missiles [16], in addition to a number of commercial satellites. After reviewing the aforementioned failures, it is evident that whiskers can pose serious problems in high-reliability systems that could result in loss of life as well as significant capital losses.

Electronics have traditionally used tin plating on leads to increase solderability and to prevent corrosion of the base metal [17]. Since the 1960s alloying the tin plating with as little as 1% lead has proven to be an effective tin whisker mitigation strategy while maintaining desirable qualities such as good solderability, low cost, appearance, and ease of plating process control [18]. However, errors in process controls have allowed pure tin plating to slip through the supply chain even when it was prohibited by procurement specifications. Process escapes have resulted in tin whisker-related failures, for example the relay used in military aircraft that failed due to metal vapor arcing caused by tin whisker shorts [19]. In addition, in an effort to protect the environment, lead-free legislation such as the European Union's Reduction of Hazardous Substances (RoHS) has placed restrictions on the use of lead and other hazardous materials [20]. To comply with RoHS and other lead-free legislation, many manufacturers have converted to pure tin finishes. Given that the spacing between leads in electronics continues to decrease as well as the proliferation of pure tin finishes, improving our ability to assess the risk associated with tin whiskers remains an important area of study.

II. Background

An application-specific tin whisker risk algorithm was developed by Pinsky of Raytheon in 2003 [21]. This risk assessment

Manuscript received June 26, 2007; revised August 24, 2007. This document was prepared under the sponsorship of the National Aeronautics and Space Administration. Neither the United States government nor any person acting on behalf of the United States government assumes any liability resulting from the use of the information contained in this document, or warrants that such use will be free from privately owned rights. This work was supported in part by S. M. Poulos, J. N. Cowart, A. Oliu, and S. J. McDanels of the National Aeronautics and Space Administration. This work was recommended for publication by Associate Editor R. Gedney upon evaluation of the reviewers comments.

K. J. Courey is with the Orbiter Sustaining Engineering Office, National Aeronautics and Space Administration, Lyndon B. Johnson Space Center, Kennedy Space Center, FL 32899 USA (e-mail: karim.j.courey@nasa.gov).

S. S. Asfour is with the Department of Industrial Engineering, University of Miami, Coral Gables, FL 33146 USA (e-mail: sasfour@miami.edu).

J. A. Bayliss, L. L. Ludwig, and M. C. Zapata are with the Materials Science Division, National Aeronautics and Space Administration, Kennedy Space Center, FL 32899 USA (e-mail: jon.a.bayliss@nasa.gov; lawrence.l.ludwig@nasa.gov; maria.c.zapata@nasa.gov).

Color versions of one or more of the figures in this paper are available online at http://ieeexplore.ieee.org.

Digital Object Identifier 10.1109/TEPM.2007.914210

1521-334X/$25.00 © 2008 IEEE

considers the following factors: conductor spacing, lead content in tin plating, process by which the tin was deposited, tin thickness, material directly beneath the tin, substrate controlling the coefficient of thermal expansion, thermal treatments the tin was subjected to after deposition, conformal coating over the tin, use of mechanical hardware, vulnerability of the system to dysfunction as a result of the presences of small pieces of conductive contaminants, use of conformal coating on conductors in the enclosure, and air flow in the assembly. The purpose of this algorithm was to quantify the risk that tin whiskers will bridge between conductors for a specific tin plating application.

In 2005, Hilty and Corman of Tyco Electronics developed a Monte Carlo simulation tin whisker reliability assessment [22]. The purpose of their work was "to help predict the likelihood for electrical shorting between adjacent leads of a typical component." Tin whiskers were grown on two different samples. The first was a plating and substrate selection that had been proven to grow whiskers; the second utilized a plating process and substrate shown to mitigate whisker growth. After exposing both of these samples to the same accelerated aging environment, the quantity, length, and growth density were measured. This data was used to fit the statistical distributions that were utilized by the simulation to determine whisker length. The locations of the whiskers, the rotation, and inclination angles were randomly generated in the simulation. Whiskers that were long enough and grew at an angle that allowed them to touch an adjacent contact were identified as a failure for the component. The results of the simulations provide a quantitative assessment of the effectiveness of plating process mitigation in reducing simulated failure rates, as well as the effect of terminal separation distance. This was the first application of a Monte Carlo simulation for tin whisker risk assessment.

In October 2005, the second tin whisker risk assessment using Monte Carlo simulation was published by Fang at the University of Maryland [23]. In addition to developing a simulation to predict the risk of an electrical short from a tin whisker growth from a conductor to an adjacent conductor, this study also developed a simulation to assess the risk of shorts from free whiskers. The author attributed the large difference between the experimental results and the results of the simulation for free whiskers to contact resistance. In the Recommendations for Future Work Section, Fang stated "In order to obtain a more accurate simulation answer, it is recommended to quantify the probability of occurrence of an electrical short given a whisker bridging adjacent exposed conductors physically. This number will be used as an input data to the algorithm to correct the final bridging simulation risk."

In the aforementioned simulations, it is assumed that physical contact between a whisker and an exposed contact results in an electrical short. This conservative assumption has been made because the probability of an electrical short from tin whiskers has not yet been determined. The purpose of our experiments was to quantify the probability of an electrical short when a whisker bridges two adjacent exposed electrical contacts.

Contact resistance is the sum of the constriction resistance and the film resistance [24]. When two surfaces touch, only a small portion of the area actually makes contact due to unevenness in the surfaces. The a-spot is the radius of the circular contact area. Current flow is constricted through the smaller area resulting in a constriction resistance. Film resistance is due to the build up of tarnish films (oxides, etc.) on the contact surfaces that act in a nearly insulating manner.

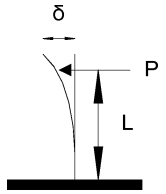

Fig. 1. Cantilever beam whisker model illustrating the mechanical load placed on a whisker by the micromanipulator probe.

Slade [25] points out that when the ratio of $(\rho_f/\rho)\,(d/a)$ is much larger than unity, the effect of constriction resistance is overshadowed by the film resistance, where ρ_f = the resistivity of the film, ρ = the resistivity of the substrate material, d = the film thickness, a = the a-spot, radius.

Contact resistance can be measured by putting two metal cylinders in contact with each other in a crossed arrangement under a mechanical load and measuring the current through the crossed rods and the voltage across the crossed rods [26]. The a-spot radius can be estimated with the crossed cylinder model developed by Holm as shown in (1.1). This assumes that the whiskers are cylindrical which is a simplification since whiskers are fluted.

$$a = 1.11\sqrt[3]{\left(\frac{P}{E}\right)r}. \tag{1.1}$$

In (1.1), P = the mechanical load, E = the modulus of elasticity, r = the radius of crossed rods, and a = the radius of the contact surface [26]. The tip of the micromanipulator which is used to make contact with the tin whiskers is also called the probe. The mechanical load of the probe touching the whisker can be estimated by modeling the whisker as a cantilever beam as shown in Fig. 1.

The whisker bending model also assumes that the whiskers are cylindrical. With that assumption stated, P = the force applied to the whisker, L = the distance from the base of the whisker to the applied force, δ = the whisker deflection, I = the moment of inertia, and E = the modulus of elasticity [27]:

$$P = \frac{3EI\delta}{L^3}. \tag{1.2}$$

The moment of inertia for a circular section is shown as follows [27]:

$$I = \frac{\pi r^4}{4}. \tag{1.3}$$

If we assume a whisker has a diameter of 2 μm, length of 4 mm, the probe contacts the whisker at 80% of its length (L = length of whisker $\times$ 0.80), and it deflects 5% of its length (δ = length of whisker $\times$ 0.05), then using (1.3) the moment of inertia $I = 7.854$ E-25 m^4. Given that the modulus of elasticity for tin is $E = 41.369$ GPa [28], using (1.2), the force applied to the whisker $P = 5.949$E-10 N. Since we have calculated a

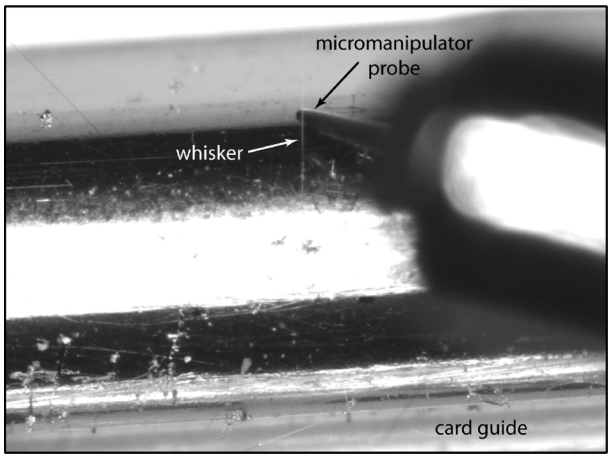

Fig. 2. Micromanipulator probe touching tin whisker number 20 growing from the card guide.

value for P, we can determine the spot area radius using (1.1), resulting in the value $a = 2.689\text{E-}9$ m.

Since the resistivity of tin at 20 °C is $\rho = 11.6\text{E-}8\ \Omega\text{m}$ [25], and the resistivity of tin oxide at 20 °C is $\rho_{\text{oxide}} = 4\text{E}4\ \Omega\text{m}$ [29], if we assume the oxide film thickness is $d = 50$ Å [30], the ratio of $(\rho_f/\rho)\,(d/a) = 6.412\text{E}11$. Since the aforementioned ratio is much larger than unity, we can conclude the effect of constriction resistance is overshadowed by the film resistance.

In order to determine the probability of an electrical short from a tin whisker across adjacent exposed leads it is necessary to determine when the film resistance from the oxide layer and any other films breaks down. Conduction can be experienced when the film is ruptured mechanically in some spots, as in a switch with wiping action contacts, or is electrically broken down when enough voltage is applied. This type of breakdown is called fritting [24]. The breakdown voltage can be seen by examining the change in the plots of the whisker voltage and whisker current.

III. Experimental Procedures

To determine the breakdown voltage, a micromanipulator probe was brought in contact with the side of a tin whisker growing from a tin-plated beryllium copper card guide as illustrated in Fig. 2. The card guide used in this experiment was removed from a Space Shuttle Orbiter Flight Control System (FCS) Ascent Thrust Vector Control (ATVC) Line Replaceable Unit (LRU) that was built in 1989.

A PXI automated data acquisition (DAQ) system was used to ensure improved experimental control. PXI is a platform for measurement and automated systems that uses a personal computer (PC) [31]. The acronym PXI stands for (PCI eXtensions for Instrumentation). Peripheral component interconnect (PCI) is a specific type of bus that is used in PCs for connecting peripheral devices to the motherboard of the PC [32].

DAQ software was written using LabVIEW to automate both the incrementing of power supply voltage changes as well as the gathering of the voltage and current data for each of the tin whiskers. Once contact was established, as determined with an optical microscope, the power supply voltage was increased from 0 to 45 Vdc in 0.1 Vdc increments. Fig. 3.

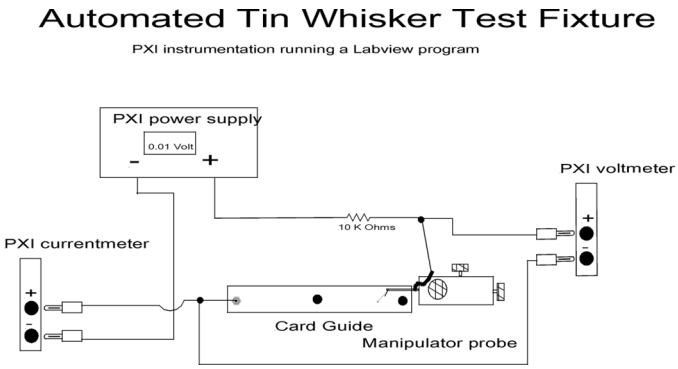

Fig. 3. Cable interconnect diagram for the tin whisker test station instrumentation.

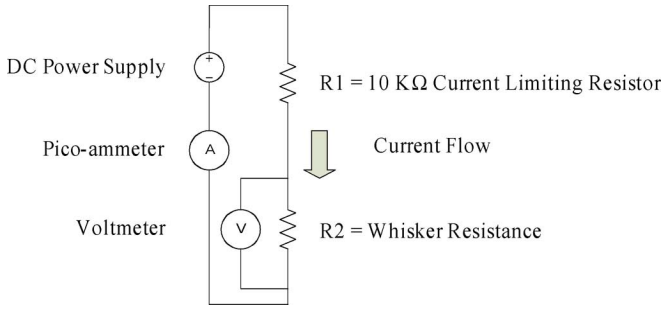

Fig. 4. Electrical schematic for the tin whisker test station.

The software captured three to four samples per second over the entire voltage range. The whisker voltage measurement included the resistance of the micromanipulator probe and lead as well as the card guide. However, the resistance of the whisker prior to film breakdown is so high, and the lead/probe resistance and the card guide are so low, that they can be represented as a single resistance value, $\text{R}2 =$ whisker resistance, in the simplified electrical schematic illustrated in Fig. 4. To avoid vaporizing the whiskers, a 10-kΩ resistor was placed in series with the whisker to limit the current through the whisker when the break down voltage was achieved. With the current-limiting resistor in place, the test station was limited to a maximum of 4.5 mA at 45 Vdc. The automated test fixture was validated by substituting a calibrated resistor decade box for the micromanipulator, whisker and card guide. The experiment was repeated to develop an empirical probability distribution of shorting as a function of voltage.

IV. Experimental Results

A. Contact Resistance

The point at which a short occurs, when the film resistance breaks down, can easily be seen in Fig. 6 when the current jumps from near zero, the nanoamp range, to the milliamp range.

Prior to breakdown, the majority of the voltage drop is across the whisker due to the high resistance of the oxide film on the whisker. In this state, the whisker voltage reading tracks close to the power supply voltage. The power supply voltage increases linearly from 0 to 45 Vdc, then it remains at 45 Vdc for a few seconds at the end of the run until the software is given a stop command. After the film has broken down, the majority of the

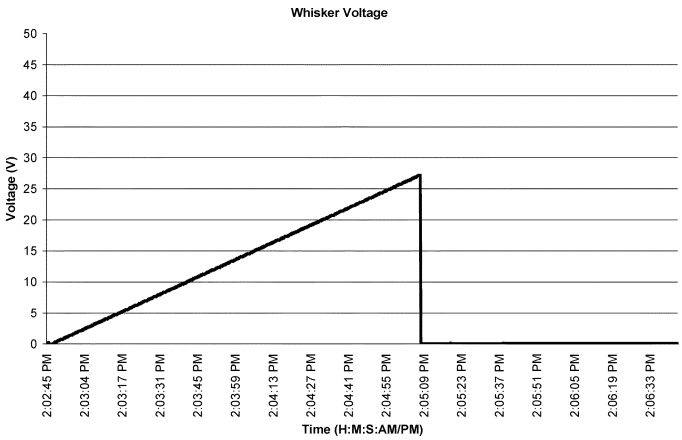

Fig. 5. Whisker voltage as a function of time plotted for whisker number 32, illustrating a single transition point.

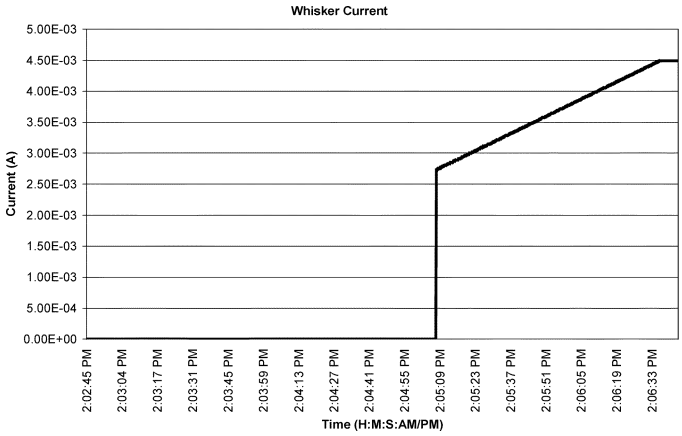

Fig. 6. Whisker current as a function of time plotted for whisker number 32, illustrating a single transition point.

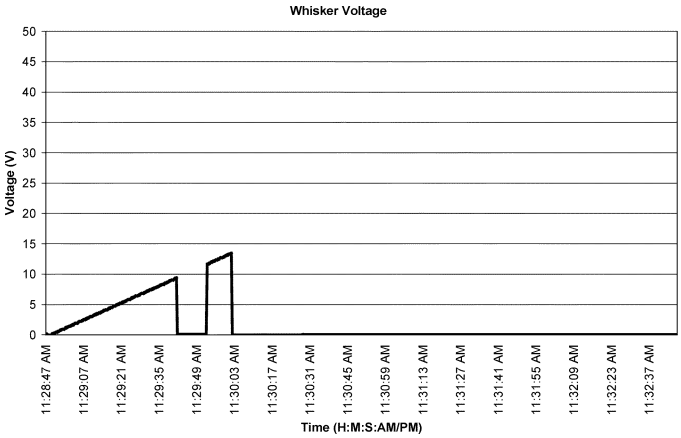

Fig. 7. Whisker voltage as a function of time plotted for whisker number 4, illustrating multiple transition points.

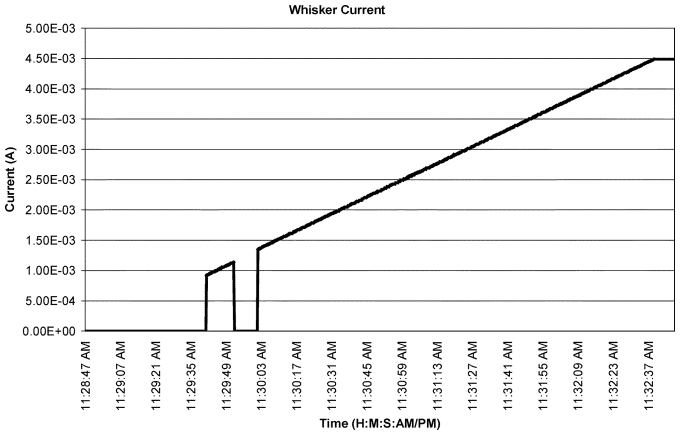

Fig. 8. Whisker current as a function of time plotted for whisker number 4, illustrating multiple transition points.

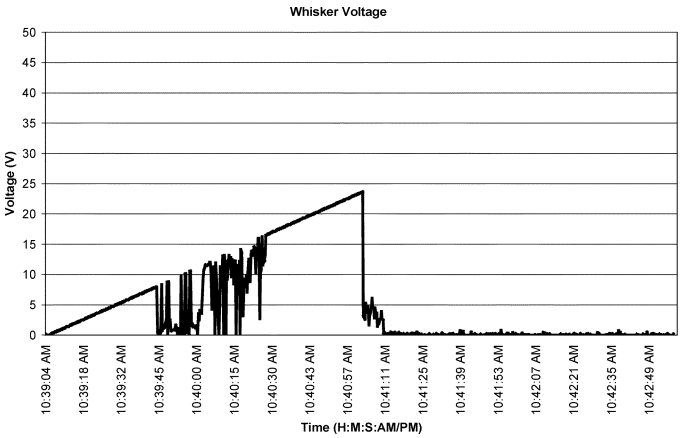

Fig. 9. Whisker voltage as a function of time plotted for whisker number 2, illustrating multiple transition points with intermittent contact.

voltage drop is across the current-limiting resistor. In this state, the low whisker voltage reading determined the small resistance of the whisker, card guide, and micromanipulator. Refer to Figs. 4 and 5.

Although the software had originally been written to stop recording data after the film resistance broke down as determined by the change in whisker current, it was decided to run 35 whiskers to the full range of the test, 0 – 45 Vdc, to observe their behavior.

An interesting benefit of running the test from 0 – 45 Vdc for all of the whiskers was the opportunity to witness the difference in transitions. A single transition point, as illustrated in Figs. 5 and 6, was exhibited by 20 of the 35 whiskers tested. Multiple transition points, as shown in Figs. 7 and 8, were found in nine of the 35 whiskers tested.

Multiple transitions with intermittent contact were present in six of the 35 whiskers tested. The intermittent contact may be explained by air currents in the room. Whiskers are very flexible and can appear to move like grass in the wind when observed under a microscope. Other possible explanations are that the probe was barely making contact with the whisker, or that thermal expansion caused whisker movement. An example of multiple transitions with intermittent contact is shown in Figs. 9 and 10.

For the tin whiskers that exhibited multiple transitions and multiple transitions with intermittency, the first occurrence of breakdown was recorded as the breakdown voltage for the whisker. This was chosen because the first time the whisker conducts current in the milliamp range it can cause a short

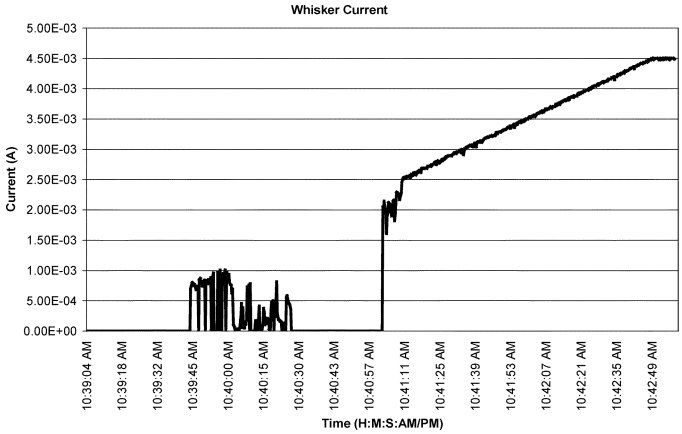

Fig. 10. Whisker current as a function of time plotted for whisker number 2, illustrating multiple transition points with intermittent contact.

TABLE I
TIN WHISKER BREAKDOWN VOLTAGE DATA

Whisker Number	Transitions[a]	Whisker Voltage
1	S	33.57
2	M/I	7.99
3	M/I	3.39
4	M	9.29
5	M	3.08
6	M	15.68
7	S	13.48
8	S	8.49
9	M/I	13.57
10	S	2.09
11	M/I	10.69
12	S	1.89
13	S	10.09
14	M	28.17
15	M/I	8.38
16	M	4.29
17	M	29.27
18	S	38.96
19	S	18.09
20	S	22.49
21	S	22.49
22	S	18.89
23	S	5.09
24	M	9.59
25	S	5.68
26	M/I	8.48
27	S	28.48
28	S	4.58
29	S	44.05
30	M	8.89
31	M	8.79
32	S	27.18
33	S	14.79
34	S	21.28
35	S	34.77

[a] The abbreviations in the transitions column are defined as follows: S = single transition, M = multiple transitions, M/I = multiple transitions with intermittant contact

circuit. The breakdown voltages for all 35 whiskers are summarized in Table I.

The whiskers 17 and 24 conducted up to 3.06 and 2.00 mA, respectively, before metallic conduction ceased. This result is likely caused by either vaporization of the whisker, or the whisker slipping away from the micromanipulator tip because the whisker was being touched too close to the end of the micromanipulator probe.

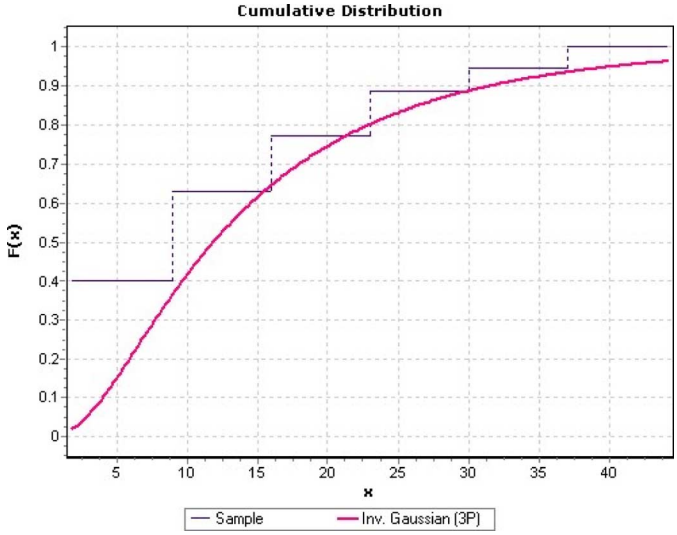

Fig. 11. Cumulative distribution of sample data and inverse Gaussian (three-parameter) model as a function of voltage.

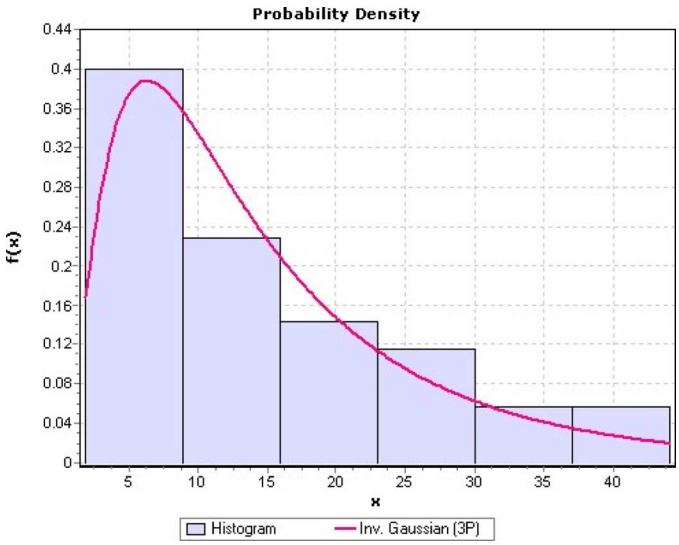

Fig. 12. Probability density function of inverse Gaussian (three-parameter) model as a function of voltage with a histogram of the sample data.

The voltage level at the transition to metallic conduction current is the voltage level at which the film and oxide layers break down. The data is a table of breakdown voltage for each specimen.

From the data in Table I, a cumulative distribution of the fraction of whiskers that have broken down versus applied voltage is shown in Fig. 11 as a stair step shaped plot.

The smoothed idealization of this is a cumulative probability function $F(x)$, estimating the probability that the whisker contact resistance, interrogated this way, will break down when the applied voltage has a given value. Then $f(x) = dF(x)/dx$ is the probability density for breakdown at x [33]. The applied voltage is represented here by the variable x. The breakdown voltages recorded above were analyzed using EasyFit distribution fitting

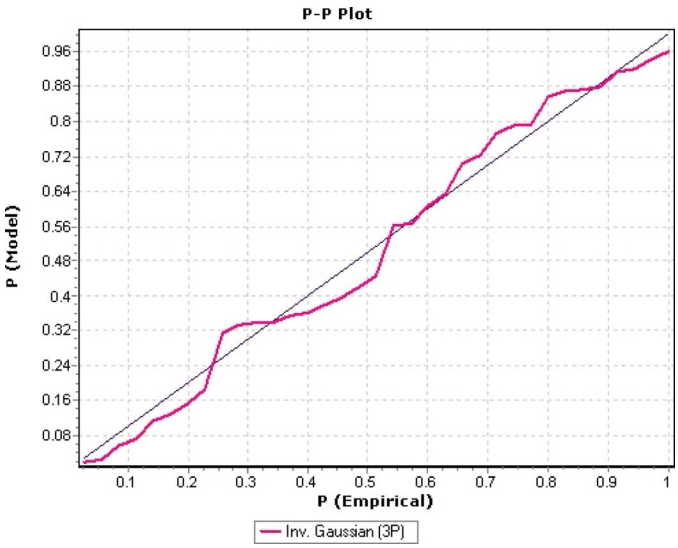

Fig. 13. Probability–probability (P–P) plot shows how well the data follows the Inverse Gaussian (threeParameter) distribution.

TABLE II
KOLMOGOROV–SMIRNOV TEST

Sample Size	35
Statistic	0.06676
Rank	1

α	Critical Value	Reject?
0.2	0.18086	No
0.15	0.1927	No
0.1	0.20622	No
0.05	0.22988	No
0.01	0.27552	No

software to determine the probability distribution that best fits the data. The best fit cumulative probability function and probability density function are shown in Figs. 11 and 12, respectively. The best fit distribution was the inverse Gaussian (three-parameter). A histogram of the data is also shown in Fig. 12.

One tool to determine how well a specific model fits the observed data is the P–P plot shown in Fig. 13. The closer the plot is to being linear, the better the model fits the observed data [34]. While the P–P plots help us weed out the distributions that do not fit well, it is often difficult to discern between the good fitting models when the plots are close in the degree of deviation from linearity. The Kolmogorov–Smirnov test will help us further analyze the best fit.

The results of the Kolmogorov-Smirnov goodness of fit test are shown in Table II. The null and alternative hypotheses for this test are: H_0: The data follows the specified distribution, H_A: The data does not follow the specified distribution [34]. At the specified level of significance α, if the test statistic is greater than the critical value, the null hypothesis is rejected. For the values of α given below, we do not reject the null hypothesis.

The EasyFit distribution fitting software tested over 40 different distributions before selecting the three-parameter inverse Gaussian as the best fit based on the Kolmogorov–Smirnov test results.

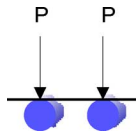

Fig. 14. Load applied to whisker lying across two conductors.

The parameters for the three-parameter inverse Gaussian distribution are $\lambda = 31.977, \mu = 17.571, \gamma = -1.9716$. The probability density function for the three-parameter inverse Gaussian distribution is shown as follows [34]:

$$f(x) = \sqrt{\frac{\lambda}{2\pi(x-\gamma)^3}} \exp\left(-\frac{\lambda(x-\gamma-\mu)^2}{2\mu^2(x-\gamma)}\right). \quad (1.4)$$

The cumulative distribution function for the three-parameter inverse Gaussian distribution is shown as follows, where $\Phi()$ is the normal cumulative distribution function [34]:

$$F(x) = \Phi\left(\sqrt{\frac{\lambda}{x-\gamma}}\left(\frac{x-\gamma}{\mu} - 1\right)\right) + \Phi\left(-\sqrt{\frac{\lambda}{x-\gamma}}\left(\frac{x-\gamma}{\mu} + 1\right)\right) \exp\left(\frac{2\lambda}{\mu}\right). \quad (1.5)$$

Based on our data, the expected (mean) voltage where a short will occur for the three-parameter inverse Gaussian distribution is $\mu - \gamma = 15.5994$ Vdc, with a variance of $\mu^3/\lambda = 169.6491$ [35].

It is important to note this distribution brings us closer to understanding the probability of a free whisker shorting across two exposed contacts. We have demonstrated that whisker shorting can be represented as a function of breakdown voltage. However, it is important to consider the limitations of the experiment including the small sample size, the number of conducting surfaces, and the difference and variation between force applied by gravity and the force applied by the micromanipulator probe.

Given that the density of tin is 7300 kg/m^3 [25], for a whisker that has a diameter of 2 μm, length of 4 mm, the whisker volume will be 1.25E-14 m^3. The whisker volume multiplied by the density of tin gives the whisker mass of m = 9.17E-11 kg. Since $F = ma$ and $a = 9.806$ m/s^2 [36], we can calculate the force of gravity on the whisker to be $F = 9.0$E-10 N. Since load applied to a whisker at each point of contact, $P = F/2 = 4.50$E-10 N as illustrated in Fig. 14.

The force applied by the micromanipulator probe to the whisker was calculated above as $P = 5.95$E-10 N. The force applied to the micromanipulator was greater that that applied by gravity $P = 4.50$E-10 N. The additional pressure was not enough to physically breach the oxide layer or we would have had breakdown voltages much closer to 0 Vdc. However, the difference in pressure could cause a shift in the mean of the distribution. A larger sample experiment with additional experimental controls will be performed in our future work.

B. Focused Ion Beam (FIB) Analysis

Tin whiskers from the same card guide used in the breakdown voltage experiment were cross sectioned using an FEI 200 TEM

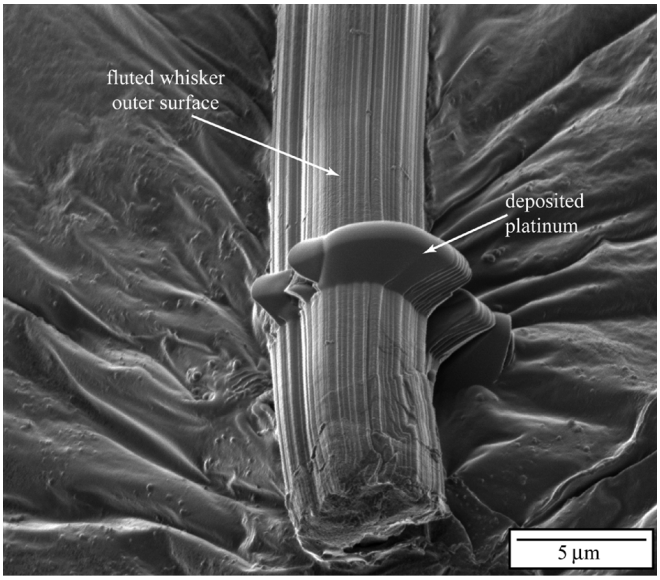

Fig. 15. FIB image of tin whisker removed from card guide shows a fluted outer surface. Platinum was deposited on the surface prior to sectioning in order to preserve the region of interest (NASA/UCF).

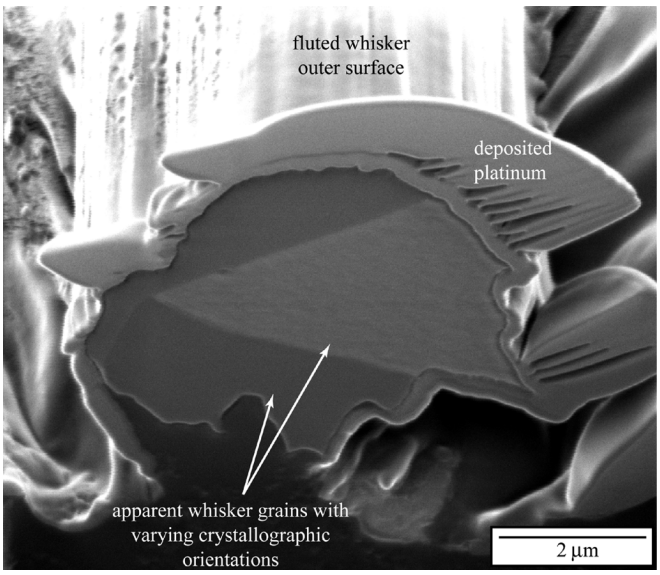

Fig. 16. FIB image of as-sectioned tin whisker shows apparent variation in grain orientation within the cross section. Image was taken at a 52° angle from horizontal (NASA/UCF).

FIB with a 30-kV gallium liquid metal ion source. The whiskers were removed from the card guide, placed on a microscopy stub using carbon tape, and then sputter coated with gold-palladium. Platinum was deposited on the region of interest prior to FIB sectioning in order to preserve the whisker's outer surface. It was observed that the whisker exhibited a fluted shape resembling an extruded surface, as shown in Fig. 15. The ion beam was used to mill away whisker material until the desired region of interest to obtain a cross section normal to the whisker's growth direction, Fig. 16.

The FIB cross section facilitates the examination of what appears to be grains with varying crystallographic orientations

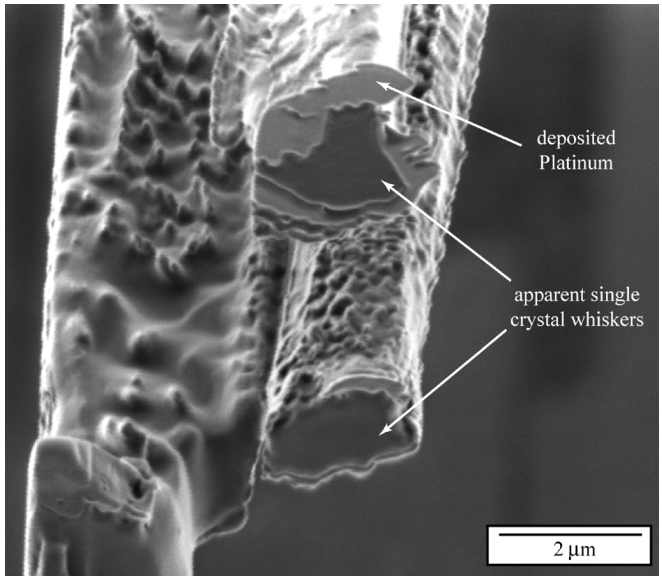

Fig. 17. FIB image of two as-sectioned tin whiskers that exhibited the expected single-crystal cross section. Image was taken 52° from horizontal (NASA/UCF).

within the tin whisker as illustrated in Fig. 16. The polycrystalline nature of the whiskers will be verified in the Part II experiment using transmission electron microscopy (TEM). The image in Fig. 16 was taken at a 52° tilt resulting in the semi-elliptical shape. However, the geometry of the cross section is expected to be more circular. The diameter of the tin whisker is approximately 6.7 μm in the vertical direction and 6.1 μm in the horizontal direction.

An additional two whiskers from the card guide were removed and sectioned by the FIB. These smaller diameter whiskers exhibited the commonly reported single-crystal structure as shown in Fig. 17. The diameter of the top whisker is approximately 2.4 μm in the vertical direction and 2.0 μm in the horizontal direction. The diameter of the bottom whisker is approximately 1.7 μm in the vertical direction and 2.0 μm in the horizontal direction. Since the cross section of the each tin whisker was not truly circular, the diameter measurements given above were made along the largest dimension in the stated direction.

V. Conclusion

In this experiment, we developed an empirical probability model to quantify the probability of occurrence of an electrical short circuit from tin whiskers as a function of voltage. This model can be used to improve existing risk simulation models. We also obtained FIB images of a tin whisker with what appears to have two different crystal orientations. Our planned future work includes a larger sample experiment to improve the probability model, as well a TEM examination of the whisker to verify the different crystal orientations in a single whisker.

Acknowledgment

The authors would like to thank Dr. H. Leidecker of NASA and J. Brusse of Perot Systems at Goddard Space Flight Center for sharing their vast knowledge on the topic of tin whiskers,

and taking the time to answer the many questions posed throughout this experiment including, but not limited to, the whisker bending model, the use of a micromanipulator for whisker probing, and oxide breakdown theory. We would also like to thank Z. Rahman, with the Materials Characterization Facility, AMPAC, University of Central Florida (UCF) for his expertise in FIB operation, M. Spates of NASA Kennedy Space Center for fabricating the test fixtures, L. Batterson of NASA Kennedy Space Center for his expertise in photography and digital imaging, S. Nerolich of United Space Alliance for his help with the cantilever beam model, M. Madden of United Space Alliance for his assistance with probability model evaluation, and Dr. A. Onar of St. Jude Children's Research Hospital for her critique of this article, and her expertise in statistics.

REFERENCES

[1] S. E. Koonce and S. M. Arnold, "Growth of metal whiskers," *J. Appl. Phys.*, vol. 24, pp. 365–366, 1953.

[2] G. T. Galyon, "Annotated tin whisker bibliography and anthology," *IEEE Trans. Electron. Packag. Manuf.* , vol. 28, pp. 94–122, Jan. 2005.

[3] H. L. Cobb, "Cadmium whiskers," *Monthly Rev. Amer. Electroplaters Soc.*, vol. 33, pp. 28–30, Jan. 1946.

[4] K. G. Compton, A. Mendizza, and S. M. Arnold, "Filamentary growths on metal surfaces—Whiskers," *Corrosion*, vol. 7, pp. 327–334, Oct. 1951.

[5] P. Harris, "The growth of tin whiskers," *Int. Tin Res. Inst.*, pp. 1–19, 1994.

[6] H. Leidecker and J. Brusse, Tin whiskers: A history of documented electrical system failures—A briefing prepared for the Space Shuttle program office 2006 [Online]. Available: http://nepp.nasa.gov/whisker/reference/tech_papers/2006-Leidecker-Tin-Whisker-Failures.pdf

[7] K. Nishimi, "Space shuttle program tin whisker mitigation," in *Int. Symp. Tin Whiskers*, 2007, pp. 1–16.

[8] Y. Hada, O. Morikawa, and H. Togami, "Study of tin whiskers on electromagnetic relay parts," in *Proc. 26th Relay Conf.*, Apr. 25–26, 1978, pp. 1–9.

[9] J. Brusse, G. Ewell, and J. Siplon, "Tin whiskers: Attributes and mitigation," in *Proc. Capacitor Resistor Technol. Symp.*, 2002, pp. 67–80.

[10] H. Leidecker, J. Brusse, M. Sampson, and J. Kadesch, NASA Goddard Space Flight Center Tin Whisker (and Other Metal Whisker) Homepage 2006 [Online]. Available: http://nepp.nasa.gov/whisker/

[11] FDA ITG Page. Tin whiskers—Problems, causes, and solutions 1986 [Online]. Available: http://www.fda.gov/ora/inspect_ref/itg/itg42.html

[12] J. Downs, "The phenomenon of zinc whisker growth and the rotary switch (or, how the switch industry captured the abominable snowman)," *Metal Finishing*, pp. 23–25, Aug. 1994.

[13] P. Daddona, "Reactor shutdown: Dominion learns big lesson from a tiny 'tin whisker'," *The Day*, Jul. 4, 2005.

[14] J. Brusse and M. Sampson, "Zinc whiskers: Hidden cause of equipment failure," *IEEE IT Professional*, vol. 6, no. 6, pp. 43–47, Nov./Dec. 2004.

[15] B. D. Nordwall, "Air force links radar problems to growth of tin whiskers," *Aviation Week Space Technol.*, vol. 124, p. 65, 1986.

[16] "The trouble with tin: Get the lead out!" Anoplate, 2000 [Online]. Available: http://www.anoplate.com/news/pastnews/fall2000/tin.htm

[17] Y. Nakadaira, T. Matsuura, M. Tsuriya, D. V. Nhat, R. Kangas, J. Conrad, B. Sundram, K. -. Lee, and S. M. Arunasalam, "Pb-free plating for peripheral/leadframe packages," in *Proc. 2nd Int. Symp. EcoDesign'01*, 2001, pp. 213–218.

[18] S. M. Arnold, "Repressing growth of tin whiskers," *Plating*, vol. 53, pp. 96–99, 1966.

[19] G. Davy, "Relay failure caused by tin whiskers," *Northrop Grumman Electron. Syst. Tech. Article*, vol. 2006, Oct. 2002.

[20] European Union, "Directive 2002/95/EC Of The European Parliament and of The Council of 27 Jan. 2003 on the Restriction of the use of Certain Hazardous Substances in Electrical and Electronic Equipment," *Official J. Eur. Union* Feb. 13, 2003, pp. L 37/19–L 37/23 [Online]. Available: http://eur-lex.europa.eu/LexUriServ/site/en/oj/2003/l_037/l_03720030213en00190023.pdf

[21] D. Pinsky, "Tin whisker application specific risk assessment algorithm," 2002 [Online]. Available: https://www.reliabilityanalysislab.com/tl_dp_0312_TinWhiskerRiskAssessmentAlgorithm.asp

[22] R. D. Hilty and N. E. Corman, "Tin whisker reliability assessment by Monte Carlo simulation," in *Proc. IPC/JEDEC Lead-Free Symp.*, 2005.

[23] T. Fang, "Tin whisker risk assessment studies," 2005, DAI-B 66(12).

[24] R. Holm and E. Holm, *Electric Contacts Theory and Application*, 4th ed. New York: Springer-Verlag, 1967.

[25] P. G. Slade, *Electrical Contacts Principles and Applications*, 1st ed. Boca Raton, FL: CRC, 1999, p. 1073.

[26] E. Holm, "Introductory lecture on fundamentals," in *Proc. Eng. Seminar Elect. Contact Phenomena*, 1962, pp. 1–13.

[27] S. Timoshenko and D. H. Young, *Elements of Strength of Materials*, 5th ed. New York: Van Nostrand Reinhold, 1968, p. 377.

[28] C. Wu, V. Kumar, R. Bailey, J. Liau, F. L'Esperance, and G. Baker, *Eng. Fundamentals*, vol. 2007, p. 1, 2007.

[29] G. V. Samsonov, *The Oxide Handbook*, 1st English ed. New York: IFI/Plenum Data, 1973, p. 524.

[30] R. Schetty, "Electrodeposited tin properties and their effect on component finish reliability," *Proc. Int. Conf. Business Elect. Product. Rel. Liability*, pp. 29–34, 2004.

[31] "LabVIEW. [Electronic]. 7.1," National Instruments, 2004 [Online]. Available: http://www.ni.com/labview/

[32] "The peripheral component interconnect," Wikipedia, 2007 [Online]. Available: http://en.wikipedia.org/wiki/Peripheral_Component_Interconnect

[33] R. E. Walpole and R. H. Myers, *Probability and Statistics for Engineers and Scientists*, 4th ed. New York: Macmillan, 1989, p. 765.

[34] Mathwave, "EasyFit," 2007, vol. 3.2.

[35] I. A. Koutrouvelis, G. C. Canavos, and S. G. Meintanis, "Estimation in the three-parameter inverse Gaussian distribution," *Comput. Statist. Data Anal.*, vol. 49, pp. 1132–1147, Jun. 2005.

[36] D. Halliday and R. Resnick, *Fundamentals of Physics*, 2nd ed. New York: Wiley, 1981, p. 816.

Karim J. Courey received the B.E.E. degree in electrical engineering from Cleveland State University, Cleveland, Ohio in 1986 and the M.B.A. degree from the Florida Institute of Technology, Melbourne, in 1993. He is currently pursuing the Ph.D. degree in industrial engineering at the University of Miami, Coral Gables, FL.

He is currently a Principal Engineer with the Orbiter Sustaining Engineering Office for the National Aeronautics and Space Administration, Lyndon B. Johnson Space Center, TX. His duty location is at the John F. Kennedy Space Center, FL. He has over 20 years of experience in the Space Shuttle Program in a wide range of positions including Systems Engineer, Design Engineer, Design Engineering Manager, Logistics Engineer, and currently a Principal Engineer for Orbiter Electrical and Avionics systems. He has worked for Lockheed, Lockheed Martin, and United Space Alliance before joining NASA in 2001.

Mr. Courey is a licensed Professional Engineer in the state of Texas. He also received a NASA Johnson Space Center Fellowship to perform doctoral research at the University of Miami during the 2006–2007 academic calendar year.

Shihab S. Asfour received the B.S. and M.S. degrees in production engineering from Alexandria University, Alexandria, Egypt, in 1973 and 1976, respectively, and the Ph.D. degree in industrial engineering and psychology from Texas Tech University, Lubbock, in 1980.

He is currently a Professor and Chairman of the Industrial Engineering Department, University of Miami, Coral Gables, FL. He has over 30 years of instructional, professional, and research experience. He has been an instructor at Alexandria University, Texas Tech University, and the University of Miami. He has taught courses in statistics, manufacturing engineering, computer programming, motion and time study, man–machine systems, occupational biomechanics, work physiology, and design of experiments at the University of Miami. His professional experience includes being a consultant to industrial, service, and educational organizations including projects funded by the U.S. Navy and Bureau of Mines. He was Principal Investigator of over 55 research projects funded by Florida Power and Light, NIOSH, The U.S. Department of Energy, and the University of Miami. He has authored over 200 publications. He has 17 recent publications in both biomechanical and industrial engineering and has also supervised 18 Ph.D. dissertations.

Jon A. Bayliss received the A.S. degree in computer engineering technology from the Tampa Technical Institute, Tampa, FL, in 1979 and the B.S. degree in electrical engineering from the Florida Institute of Technology, Melbourne, in 1986.

He is currently an Electrical Engineer in the Electronic Failure Analysis Section, Engineering Directorate for the National Aeronautics and Space Administration, Kennedy Space Center, FL. He has approximately 20 years experience in testing and failure analysis of electronic/electrical flight and ground support equipment hardware used in the Space Shuttle, Space Station, and ELV specializing in the development of automated data acquisition systems with GPIB, RS-232, Ethernet and PXI electronic measurement and control instrumentation. He worked for Collins Avionics and Harris Government Systems Division before joining NASA in 1986.

Lawrence L. Ludwig received the B.S. degree in electrical engineering from the Florida Institute of Technology, Melbourne, in 1986 and the M.S. degree in engineering management from the University of Central Florida, Orlando, in 1992.

He is currently a Lead Electrical Engineer in Electronic Failure Analysis Section, Engineering Directorate for the National Aeronautics and Space Administration, Kennedy Space Center, FL. He has expertise in electrical engineering, test instrumentation hardware and software, radiographic inspection, and electronics prototyping. He specializes in materials related failure analysis, electrical/electronic systems and components failure analysis, integrated and solid-state circuit failure analysis, and electromechanical devices failure analysis. He started his technical career as a member of an Air Force Titan II launch crew in the late 1970s.

Maria C. Zapata received the B.S. degree in materials science and engineering from the University of Florida, Gainesville, in 2002 and the M.S. degree in materials science and engineering from the Pennsylvania State University, University Park, in 2005.

She is currently a Materials Engineer in the Materials Failure Analysis Section, Engineering Directorate for the National Aeronautics and Space Administration, Kennedy Space Center, FL. She performs failure analysis for ground support equipment, flight hardware, and facilities supporting the Space Shuttle, International Space Station, and Expendable Vehicles and Constellation programs. Prior to work in the aerospace industry, she worked for ExxonMobil providing metallurgical support in the Research and Engineering downstream Central Engineering Office and at the Baton Rouge refinery.